Two-dimensional microfibril angle mapping via polarization microscopy for wood classification

Y Kita[1*], S Mizuno-Tazuru[1] and J Sugiyama[1, 2*]

[1] Research Institute for Sustainable Humanosphere (RISH), Kyoto University, Gokasho, 611-0011 Uji, Japan
[2] College of Materials Science and Engineering, Nanjing Forestry University, Nanjing 210037, Jiangsu, China

[*]E-mail: kita.yusuke.46x@st.kyoto-u.ac.jp, sugiyama.junji.6m@kyoto-u.ac.jp

Abstract. A new method is presented for measuring microfibril angles (MFAs) from transverse tree sections by using polarized optical microscopy combined with a liquid-crystal tunable filter. The MFA transition analysis of tree growth rings via generalized two-dimensional correlation is proposed. The unique features of two anatomically similar Cupressaceae species, *Chamaecyparis obtusa* S. & Z. and *Thujopsis dolabrata* S. & Z. and its variant, were extracted through MFA analysis. The technique efficiently visualized MFA distributions under wide field observation and uncovered seasonal differences. Classification results of supervised models exhibited 60% accuracy, despite featureless cross-sections of the conifers. Overall, MFA is a promising index that can identify specific features of wood species.

1. Introduction

The Japanese culture has prospered in its utilization of wood resources for many purposes. In particular, two Cupressaceae species, Hinoki (*Chamaecyparis obtusa* S. & Z.) and Hiba (*Thujopsis dolabrata* S. & Z. and *Thujopsis dolabrata* S. & Z. var. *hondae*), have been extensively used because of their superior mechanical properties, processability, and durability against water and insects relative to other species. However, they have clearly different ranks with regard to construction and locality. *C. obtusa* belongs to the highest rank because of its beautiful color, cleanliness, and utility, and has thus been used for sacred places such as shrines and temples. In contrast, the inferior *T. dolabrata* and its varieties [1] have been important alternatives to *C. obtusa* and have been preferred in the Tohoku District because of their large concentration and availability. Therefore, the ability to distinguish between *C. obtusa* and *T. dolabrata* is important for understanding Japanese history, culture, and politics.

Anatomically, both trees are nearly identical with respect to the occurrence of axial parenchyma with resin-like substances tangentially aligned in latewood, as well as the gradual transition from earlywood to latewood. The only identification criterion is the shape and amount of cross-field pitting in the earlywood, which appears in the joint between the tracheid and ray parenchyma [2]. Shimaji and Itoh [3] reported that *C. obtusa* and *T. dolabrata* usually had two cupressoid-type pittings and three or four

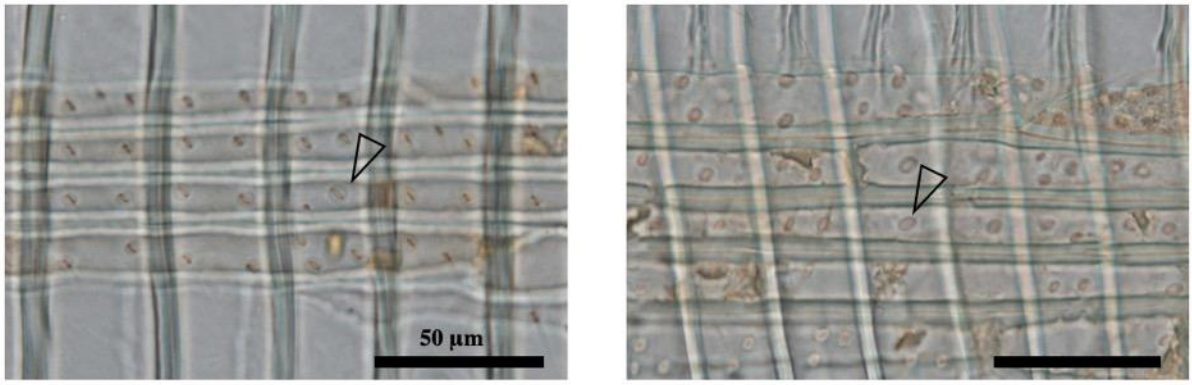

Figure 1. Optical micrographs of radial sections of *C. obtusa* (left) and *T. dolabrata* (right). The arrow heads indicate the typical cross-field pitting.

taxodioid-type pittings with some cupressoid features (Figure 1). However, Hirai [1] claimed that their shapes were categorized as cupressoid. Thus, the basis of cross-field pitting is obscure because of its dependence on experience and intuition. Noshiro (2011) statistically scrutinized the morphological aspects of cross-field pitting in Cupressaceae, including these two species, and showed possible distinguishing features [4]. Some wood anatomists rely on the occurrence of resin-like substances in ray parenchyma for a classification criterion. Consequently, a new method based on clear and quantitative criteria is needed for wood species that cannot be distinguished by conventional means.

The microfibril angle (MFA) is defined as the angle between the direction of cellulose microfibrils and the longitudinal axis in an S_2 wall. It has the potential for revealing specific features in wood species. Barnett and Bonham reported MFA differences at the family level for coniferous and deciduous species [5]. Moreover, Hori et al. [6] reported that the good acoustic properties of sitka spruce resulted from its very low MFA and small MFA differences within a growth ring. Hence, an appropriate method of determining the MFA and its seasonal differences would enable criteria for wood discrimination.

Here, a completely new method for wood classification based on MFA is discussed and applied to the identification of *C. obtusa* and *T. dolabrata*. The new method involves measuring MFA distributions from the transverse dimension of tracheids with a wide-field polarization microscope and a liquid-crystal tunable filter (LCTF) [7]. The distributions were transformed into two-dimensional MFA (2D MFA) correlation maps that reflected the degree of seasonal MFA differences within an annual ring. The maps were also inputted into multivariate classifiers, K-Nearest-Neighbor (KNN) [8] and random forest [9].

2. Materials and methods

2.1. Materials

Blocks of *C. obtusa* registered as KYOw 00638, 04431, 04436, 08005, 08007, 14105, 17823, and 17824, and blocks of *T. dolabrata* and *T. dolabrata* var. *hondae* registered as KYOw 00034, 00579, 00580, 08017, 08018, and 13581 by the xylarium at the Research Institute for Sustainable Humanoshpere, Kyoto University (http://database.rish.kyoto-u.ac.jp/cgi-bin/bmi/en/namazu.cgi) were used. Along with *T. dolabrata*, they were gifts from Prof. Takata K, No.1, No.2, and No.3. All wood samples were collected from mature and normal wood areas.

2.2. Methods

2.2.1. Sample preparation

All the wood samples were cut with a sliding microtome into 10-μm-thick cross sections. To avoid rupturing of cell walls during sectioning, the surfaces of the wood blocks were covered with a cornstarch solution [10].

2.2.2. MFA measurement from cross sections

The determination of MFAs from transverse sections via optical anisotropy of cellulose microfibrils in cell walls was developed by Abraham and Elbaum [11, 12]. The advantage of this method is greater MFA accessibility over a wide range with high resolution. The degree of birefringence or retardation in a cross section theoretically depended on the MFA. They used a Polscope system, developed by Oldenbourg and Mei [13], which could directly obtain retardation images via an electronically controlled retarder (Figure 2).

Here, instead of retardation, interference colors under polarization were used to analyze the MFAs. The spectrum of interference colors was dependent on the retardation by the fibrils. Hence, the MFA could be addressed via color information emitted from cell walls. The acquisition of spectral images containing interference colors was performed with a modified camera with a LCFT system developed from a Lyot filter (Figure 2) [14]. Color spectra could be obtained with 1-nm resolution with the electronically manipulated liquid crystal retarders sandwiched between linear polarizers in the LCTF.

In the conversion step from interference colors to MFA, the difference in ordinary and extraordinary refractive indices, Δn=0.07, was used [15]. In addition, the amount of cellulose in the cell wall was set to 50%, following the general value in S_2 of conifers [16].

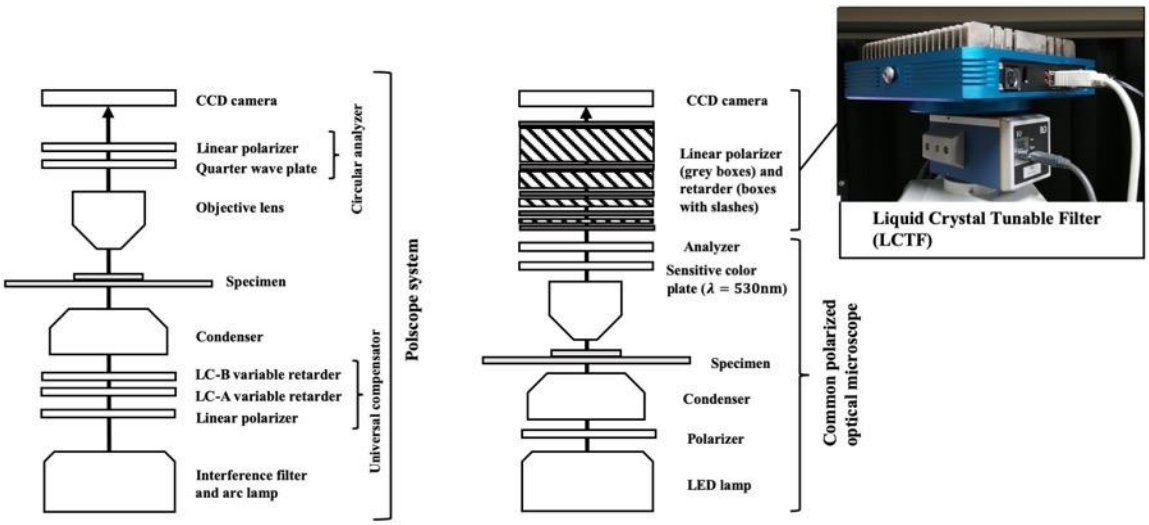

Figure 2. Schematics of a Polscope system (left) and a liquid-crystal tunable filter mounted on a polarization microscope (right).

2.2.3. Spectral imaging by LCFT

A sample cross-section was placed on the stage of a polarization microscope (Olympus BX53-P), with a sensitive color plate ($\lambda = 530$ nm) inserted under the cross-Nicol condition (Figure 3). The stage was rotated to set the radial and tangential walls parallel to the slow and fast axes, respectively. Spectral

images were taken with the LCTF (CRi VariSpec™) over the range 460–610 nm with 3-nm resolution. The magnification of the objective lens was 4× (Olympus UPLFLN-P, NA=0.13), and the exposure time was 2 s in all experiments.

2.2.4. Processing of spectral images

A flowchart of the data processing is depicted in Figure 3. Spectral images corresponding to 460–601-nm wavelength bands were transformed into MFA maps. A map was cut off in units of one growth ring; approximately 1000 MFA maps of the two species were thus obtained. The growth ring was then segmented into five sections and the MFA distribution of each section was represented by a histogram with approximately one-degree resolution. For visualizing MFA changes precisely within an annual ring, the histograms from the 0–60 degree regions were converted into two types of 2D MFA correlation maps based on season-dependent perturbations from earlywood to latewood. This required the application of generalized two-dimensional correlation spectroscopy [17], commonly used with infrared, Raman, and near infrared spectroscopy [18, 19]. 2D 60×60 maps were flattened into a one-dimensional vector with 3600 variables for inputs applicable to discrimination models.

2.2.5. Statistical analysis

Flattened synchronous and asynchronous variables (3600), and their combination (7200 variables), were randomly divided into training and test sets at a ratio of 3:1. Accordingly, six patterns of train-test set combinations were prepared to consider sample splitting.

These datasets were put into two types of classification models: KNN and random forest. In KNN, the number of neighbors for classification was set to five. In random forest, the number and depth of the trees were set to 500 and 3, respectively. The square root of all variables was adopted as the number of features for the trees.

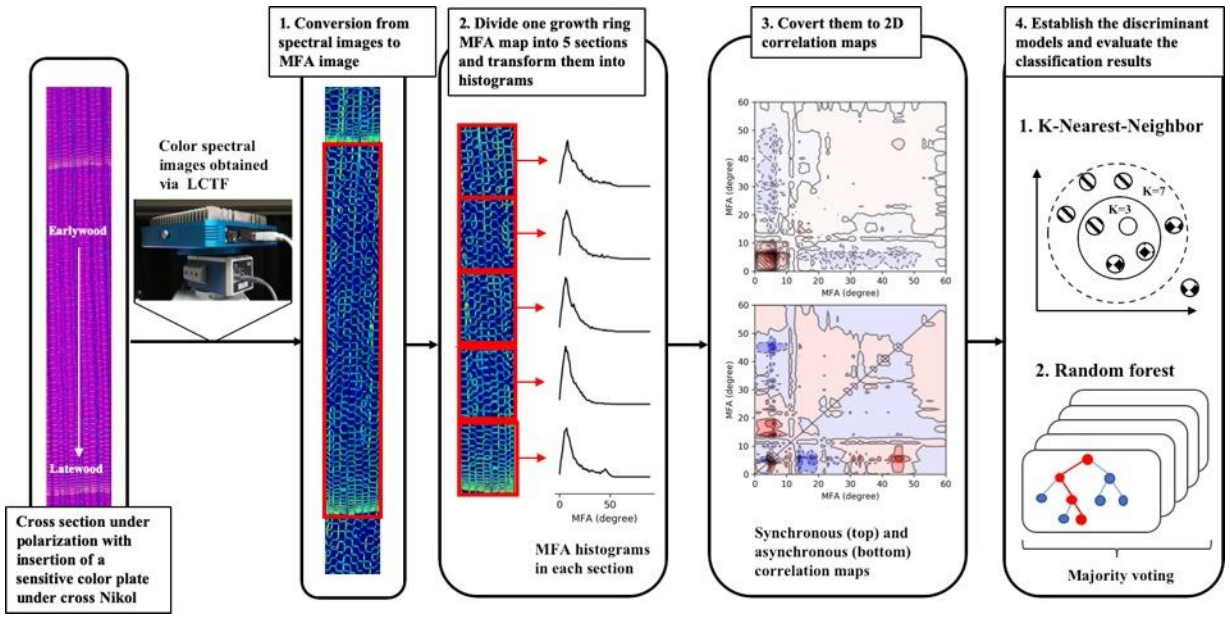

Figure 3. Experimental flowchart from data processing to classification by supervised models.

For model evaluation, five-fold stratified cross-validation [20], which creates a cross-validation dataset containing approximately the same proportions of labels as the original dataset, was conducted on the training set. Then, the classification model trained by the trained dataset was applied to the test dataset. Finally, all results obtained from each dataset were summarized and performance evaluated for

the models. In all the results, F-measure was chosen instead of accuracy in consideration of sample imbalance effects [21].

3. Results and discussion

Figure 4 shows a typical MFA map and histograms from each section. Two main peaks were observed in low (0–20 degree) and high (40–50 degree) MFA regions. They corresponded to S_2 and S_1 and peripheries of bordered pit regions, respectively. Generally, the MFA increased around pit apertures similar to the bordered pits between tracheids [22] and the cross-field pitting in the joint of tracheid and ray parenchyma [23], because a flow of cellulose microfibrils circumvented pit apertures. Here, these cell wall microstructures were successfully observed via MFA. In contrast, the orientation angle of the S_1 wall was underestimated relative to usual values of 80 degrees [16]. This was attributed to the difference in the proportion of cellulose with respect to other components in S_1 and S_2; the amounts of cellulose content in each wall were 30% and 50%, respectively [24].

The synchronous and asynchronous correlation maps of the histograms in Figure 4 are shown in Figure 5. The interpretation of the generalized two-dimensional correlation spectra followed Noda (1993) [25]. In the synchronous MFA map, the highly crowded range around 0–20 degrees was well-resolved into two main groups, 0–10 degrees and 10–20 degrees, by expansion from 1D to 2D. Autocorrelation and correlation of the lower and higher angle groups exhibited positive and negative peaks, respectively. This indicated that the two areas inversely reacted against the seasonal perturbations. Therefore, lower and higher peaks were assigned to the S2 wall in latewood and several earlywoods because the MFA gradually decreased in latewood [26].

Moreover, the combination of synchronous and asynchronous correlation spectra revealed information regarding the timing of the MFA transitions. In the lower region of 0–20 degrees, two large asymmetrical positive and negative correlation peaks appeared in the upper left and lower right sections of the asynchronous map, respectively. In contrast, only negative peaks were detected at the same positions in the synchronous map, indicating that the decrease of 10–20 degrees preceded the increase of the 0–10-degree region. The same discussion could be applied to S1 and the bordered pit regions, and to the 10–20-degree region. Accordingly, the increase of the 50-degree region predated the 0–20-degree region. Therefore, the increment of the contribution from S1, the decrement of S2 around 10–20 degrees, and the increase of S2 to 0–10 degrees, occurred

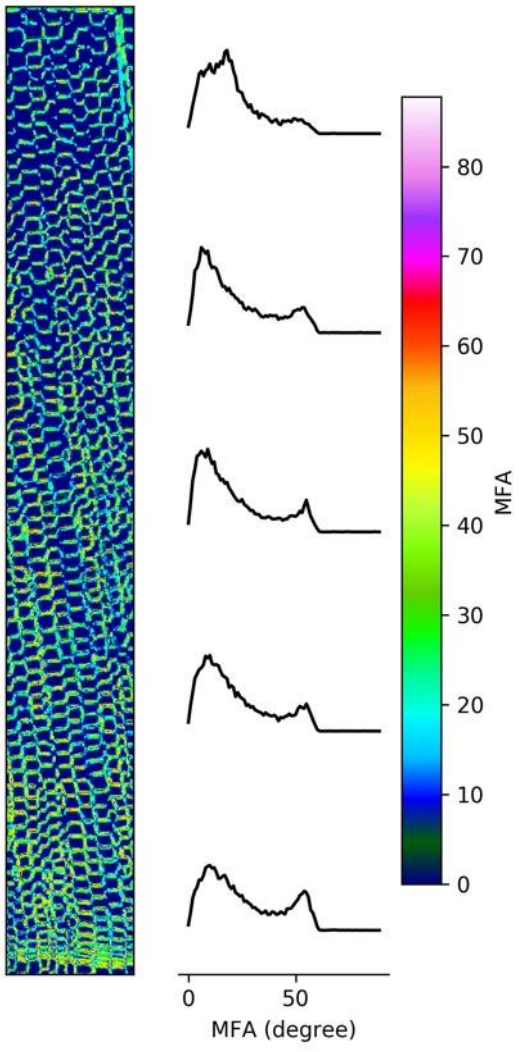

Figure 4. Typical MFA map within a growth ring (left) and MFA histograms (right), obtained from *C. obtusa* (KYOw04438).

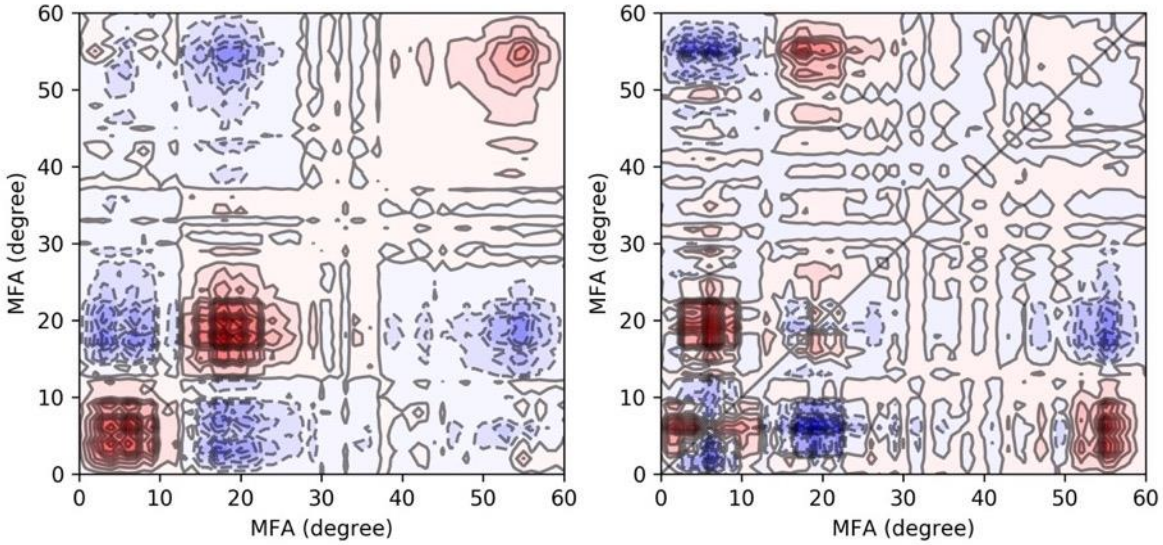

Figure 5. Typical synchronous (left) and asynchronous (right) 2D MFA correlation maps, obtained from *C. obtusa* (KYOw04438) with one-degree resolution.

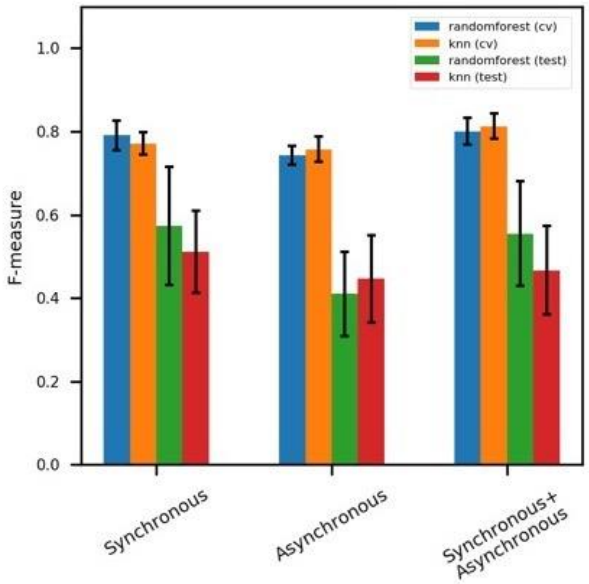

Figure 6. Mean F-measure values obtained from the KNN and random forest models. Inputs were flattened synchronous (left), asynchronous (center), and a combination (right). The error bars were standard deviations from six patterns of train-test splitting.

sequentially within a growth ring in this sample. In this way, the generalized two-dimensional correlation spectra were powerful tools for analyzing the MFA transition.

Figure 6 shows the classification result using two supervised discriminant models whose inputs were two types of flattened correlation maps and a combination of the two. The mean F-measure in the test dataset was 0.6, even for the random forest that had the best result. This indicated that the two tree species had similar MFA features and transitions within a growth ring. In addition, large standard

deviations for the test set results indicated that the training and test data splitting had a large effect on the identification accuracy. That is, there was a large variance within the same species.

4. Conclusion

In conclusion, MFA information was successfully extracted via analysis of transverse tree sections. Optical anisotropy of the cellulose fibers and generalized two-dimensional correlations were used to determine MFA transitions within growth rings. These extraction methods combined with supervised models had 60% accuracy for the identification of anatomically similar conifers. Overall, there is great potential to extract specific features of wood species from cross-sectional images.

Acknowledgements

We thank Professor Katsuhiko Takata, Akita Prefectural University, for a kind gift of *T. dolabrata* samples. This study was supported by a Grant-in-Aid for Scientific Research (18H05485) from the Japan Society for the Promotion of Science and partly by RISH cooperative research (database) and RISH Mission Research (V-4). We thank Alan Burns, PhD, from the Edanz Group (www.edanzediting.com/ac) for editing a draft of this manuscript.

References

[1] Hirai S 1996 *Encyclopedia of trees* (Tokyo: Asakura Publishing) pp 62-64
[2] Wheeler E A, Baas P and Gasson P E 2004 IAWA list of microscopic features for softwood identification *IAWA J* **25** 1
[3] Shimaji K and Itoh T 1982 *Atlas of wood structure of Japanese trees* (Tokyo: Chikyusha Press) pp 76-77
[4] Noshiro S 2011 Identification of Japanese species of Cupressaceae from wood structure *Jpn. J. Histor Bot.* **19** 125
[5] Barnett J R and Bonham V A 2004 Cellulose microfibril angle in the cell wall of wood fibres *Biol. Rev.* **79** 461
[6] Hori R, Müller M, Watanabe U, Lichtenegger H C, Fratzl P and Sugiyama J 2002 The importance of seasonal differences in the cellulose microfibril angle in softwoods in determinig acoustic properties *J. Mater. Sci.* **37** 4279
[7] Beeckman J, Neyts K and Vanbrabant P J M 2011 Liquid-crystal photonic applications *Opt. Eng.* **50** 081202
[8] Cover T M and Hart P E 1967 Nearest neighbor pattern classification *IEEE Trans. Inf. Theory* **13** 21
[9] Breiman L 2001 Random forests *Mach. Learn.* **45** 5
[10] Gärtner H *et al.* 2015 A technical perspective in modern tree-ring research -how to overcome dendrocholonological and wood anatomical challenges *J Vis Exp.* **97** 52337
[11] Abraham Y and Elbaum R 2013 Quantification of microfibril in secondary cell wall at subcellular by means of polarized light microscopy *New Phytol.* **197** 1012
[12] Abraham Y and Elbaum R 2013 Hygroscopic movements in Geraniaceae: the structural variations that are responsible for coiling or bending *New Phytol.* **199** 584
[13] Oldenbourg R and Mei G 1995 New polarized light microscope with precision universal compensator *J Microsc.* **180** 140
[14] Lyot B 1933 Optical apartus with wide field using interference of polarized light *Acad. Sci.* **197** 1593
[15] Iyer K R K, Neelakantan P and Radhakrishnan T 1968 Birefringence of native cellulosic fibers. I. Untreated cotton and ramie *J. Polm. Sci.* A-2 **6** 1747
[16] Panshin A J and Zeeuw C D 1964 *Text book of wood technology volume I- structure, identification, uses, and properties of the commericial woods of united states* (New York: McGraw Hill) pp 64-70
[17] Noda I, Dowrey A E, Marcott C, Story G M and Ozaki Y 2000 Generalized two-dimensional correlation spectroscopy *Appl. Spectrosc.* **54** 236

[18] Noda I 2014 Frontiers of two-dimensional correlation spectroscopy. Part 1. New concepts and nortworthy developments *J. Mol. Struct.* **1069** 3
[19] Noda I 2014 Frontiers of two-dimensional correlation spectroscopy. Part 2. Perturbation methods, fields of applications, and types of analytical probes *J. Mol. Struct.* **1069** 23
[20] Kohavi R 1995 A study of cross-validation and bootstrap for accuracy estimation and model selection *IJCAI'95 Proc. of the 14th international joint conf. on Artificial intelligence -Volume 2* pp 1137-1143
[21] Chincor N 1992 MUC-4 evaluation metrics *Proc. of the Fourth Message Understanding Conf.* pp 22-29
[22] Anagnost S E 2002 Variation of microfibril angle within individual tracheids *Wood Fiber Sci.* **34** 337
[23] Lichtenegger H C, Müller M, Wimmer R and Fratzl P 2003 Microfibril angles inside and outside crossfields of Norway spruce tracheids *Holzforschung* **57** 13
[24] Panshin A J and Zeeuw C D 1964 *Text book of wood technology volume I- structure, identification, uses, and properties of the commericial woods of united states* (New York: McGraw Hill) pp 71-73
[25] Noda I 1993 Generalized two-dimensional correlation method applicable to Infrared, Raman, and other types of spectroscopy *Appl. Spectrosc.* **47** 1329
[26] Donaldson L 2008 Microfibril angle: measurement, variation and relationships -a review *IAWA J* **29** 345